

Relativistic detonation waves and bubble growth in false vacuum decay

Paul Joseph Steinhardt

Department of Physics, University of Pennsylvania, Philadelphia, Pennsylvania 19104

(Received 3 November 1981)

After reviewing the current understanding of relativistic shock waves, a detailed analysis of relativistic detonation waves is presented. It is proposed that the motion of a detonation wave is analogous to the growth of a bubble nucleated during false vacuum decay at finite temperatures. Some possible applications of these results to cosmology are discussed.

I. INTRODUCTION

The relativistic theory of hydrodynamic shock waves has been well established for years.¹⁻⁴ Closely related to the shock wave is a phenomenon that takes place in a combustible medium when the combustion process is mediated by a shock wave. The fluid on the front side of the shock wave is unburnt fluid whereas the fluid on the rear side of the wave is fluid that has undergone combustion and is of different "chemistry" from the front side. When the shock wave passes some point in the unburnt fluid, the reaction begins at that point and continues until all the fluid has burned, i.e., for a time τ which characterizes the kinetics of the reaction concerned. The shock wave is therefore followed by a layer moving with it in which combustion is occurring. The width of this layer depends on the velocity of the shock and the characteristic time τ . When the dimensions in the problem are sufficiently large, one can regard the shock wave and combustion zone following it as a single surface of discontinuity which separates the burnt and unburnt fluids. The surface is referred to as the detonation wave. Relativistic detonations have not been previously analyzed in the literature.²

As the detonation wave travels, stored chemical energy in the fluid on the front side of the wave is released and is used to further propel the wave or is left as kinetic energy in fluid left behind the traveling wave front. The motion of a spherical detonation wave is therefore analogous to the growth of a bubble which is nucleated in a first-order phase transition. In the latter case, the raised potential energy of the false vacuum is converted into kinetic energy as the bubble wall passes and is used to propel the bubble wall or remains in

particles left behind the bubble wall.

Coleman⁵ has analyzed the decay of a metastable phase into a stable one for field theories *in vacuo* at zero temperature and has shown how the decay process occurs through the nucleation of bubbles containing a stable phase. Once nucleated, an isolated bubble grows, accelerating indefinitely until the velocity of the wall approaches the speed of light. "All of the energy" released in the decay is used to further accelerate the bubble wall, thus leaving the center of the bubble at zero temperature and with rapidly decreasing energy. If many bubbles are produced, each grows until the walls coalesce with the growing walls of the other bubbles and the system reaches equilibrium at a temperature near the critical temperature.

Recently, there has been a great deal of interest in applying Coleman's results to understanding phase transitions in early cosmology. The problem is that in early cosmology the Universe was not a vacuum and, according to current theories of cosmology, was at a very high temperature. Linde⁶ has shown how to modify Coleman's expression for the bubble nucleation (by replacing the energy in Coleman's expression with the free energy) for high temperatures. However, there remains the question as to how the bubbles grow in a non-vacuum at high temperatures; it is important to resolve this issue in order to determine how fast the bubbles coalesce and the transition is completed.

Therefore, if the bubbles do behave like spherical detonation waves, the results that are derived in this paper provide the answers as to what the rate and manner of growth of bubbles at finite temperatures is. Since the results differ from the conventional assumptions in previous papers,⁷⁻⁹ they may

prove interesting.

In Sec. II of this paper, the theory of relativistic shock waves is reviewed with particular emphasis on issues not discussed in previous papers. In Sec. III, the methods of analysis for shock waves are extended to the case of relativistic detonation waves. In Sec. IV, the application of these results to the growth of bubbles in false vacuum decay is discussed, along with possible applications to cosmology. Some concluding remarks are made in Sec. V.

II. RELATIVISTIC SHOCK WAVES

Because detonation waves are closely related to shock waves, it is useful to review the known theory of relativistic hydrodynamical shocks. A consistent notation will be used throughout in which n is the baryon density, V is the specific volume, p is the pressure, T is the temperature, s is the entropy per baryon, e is the internal energy density, $w = e + p$ is the "enthalpy,"

$$v_s = \left(\frac{\partial p}{\partial e} \right)^{1/2} \quad (2.1)$$

is the velocity of sound relative to the fluid, and

$$u_s = v_s / (1 - v_s^2)^{1/2} \quad (2.2)$$

is the "four-velocity" of sound. (Newtonian limits of these quantities are given in Landau and Lifshitz.²) The quantity $x = w/n^2$ will be another useful variable since plots of p vs x will play a key role in the analysis. Since by the first law of thermodynamics

$$de = \frac{w}{n} dn + nT ds \quad (2.3)$$

and

$$d \left(\frac{w}{n} \right) = V dp + T ds, \quad (2.4)$$

a curve of constant entropy (a Poisson adiabat) in the p vs x plot has a tangent

$$\left. \frac{\partial p}{\partial x} \right|_s = - \left(\frac{u_s}{V} \right)^2 < 0. \quad (2.5)$$

The standard analysis of relativistic shock waves and the following description of detonation waves is valid in curved space-times as well as flat—in any theory with a metric in whose local Lorentz frames the nongravitational laws of physics assume

their standard special-relativistic forms.⁴ One considers a moving plane shock front and a particular event P through which it passes. In the neighborhood of P one introduces a local Lorentz frame in which the shock is momentarily at rest. If the shock front locally lies along the $y = z = 0$ plane, then on either side of the front the fluid travels along the x direction. (A tangential discontinuity is unstable and will not be considered in this paper. Therefore tangential flow is irrelevant to this discussion.) Taub¹ has shown that such a frame can be found.

In Fig. 1 a view of the shock front in the chosen frame is shown. Region "1" denotes the *unshocked* fluid which, in this frame, travels through the shock front towards region "2" which contains the *shocked* fluid. The velocity (with respect to c) of fluids will be denoted by β_1 for the unshocked fluid and β_2 for shocked fluid with

$$u_i = \beta_i / (1 - \beta_i^2)^{1/2} \quad (2.6)$$

representing the "four-velocity" on either side.

The laws of energy and momentum conservation must be obeyed along the shock front if the front is to reach equilibrium and travel at a constant velocity (with respect to the unshocked fluid, for example). The laws may be found by transforming the energy-momentum tensor in the local rest frame of the fluid,

$$\mathcal{T}_i = \text{diag} (p, p, p, e), \quad (2.7)$$

into the local rest frame of the shock wave and by demanding the energy and momentum be conserved across the shock front:

$$w_1 \gamma_1 u_1 = w_2 \gamma_2 u_2, \quad (2.8)$$

$$w_1 u_1^2 + p_1 = w_2 u_2^2 + p_2, \quad (2.9)$$

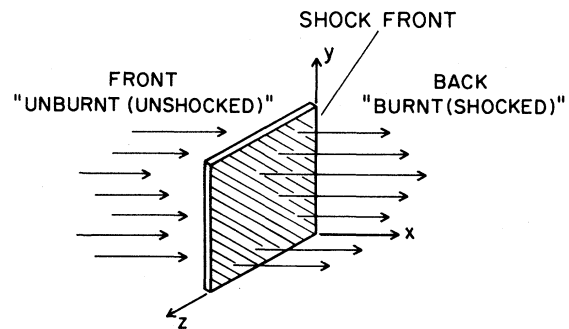


FIG. 1. A relativistic detonation (shock) wave viewed in the local Lorentz frame of the detonation front.

where

$$\gamma_1 = 1/(1 - \beta_i^2)^{1/2}. \tag{2.10}$$

(These are the \mathcal{T}_{ox} and \mathcal{T}_{xx} components.) In addition, if there is a conserved "charge" such as baryon number, one might consider the continuity relation expressing the balancing of the baryon flux:

$$n_1 u_1 = n_2 u_2 \equiv j. \tag{2.11}$$

Then, one can express the baryon flux using Eqs. (2.9) and (2.11) as

$$-j^2 = \frac{p_2 - p_1}{x_2 - x_1}. \tag{2.12}$$

By manipulating the above relations, one obtains an equation that relates (p_1, x_1) to (p_2, x_2) :

$$x_2 w_2 - x_1 w_1 = (p_2 - p_1)(x_2 + x_1). \tag{2.13}$$

One can also ignore the continuity relation and consider just Eqs. (2.8) and (2.9) to derive a relation for β_1 in terms of β_2 . In the limit of a highly relativistic fluid in which $p = e/3$, the relation has the simple form

$$\beta_1 = \begin{cases} \frac{1}{3\beta_2} & \text{for } \beta_2 \leq \frac{1}{\sqrt{3}}, \\ \beta_2 & \text{for } \beta_2 \geq \frac{1}{\sqrt{3}}. \end{cases} \tag{2.14}$$

Equations (2.8)–(2.14) are the fundamental relations governing shock-wave propagation.

To understand the utility of these relations it is useful to consider a family of shocks each with the same thermodynamic state on the "1" side but with different states on the "2" side. Given an equation of state that relates e to p , Eq. (2.13) constrains the possibilities for "2" [defined by (p_2, x_2)] to a one-parameter family which can be designated by a curve (referred to as the *Taub adiabat*) in the p vs x plane. The curve (see Fig. 2) passes through the point (p_1, x_1) . One can also show that the curve of constant entropy (the *Poisson adiabat*) which passes through "1" is tangent to the Taub adiabat at point "1" and that the two curves have the same second derivative.⁴ As the shock wave moves, there is a jump in entropy which, by the second law of thermodynamics, must be positive. Increasing entropy means that the point on the curve corresponding to fluid "2" must lie above the point (p_1, x_1) , i.e.,

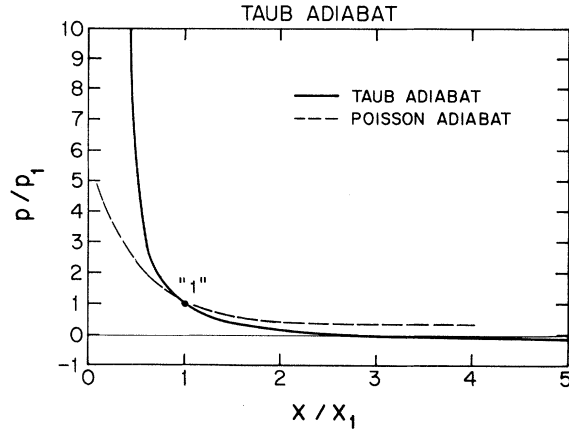


FIG. 2. The Poisson adiabat and Taub adiabat plotted in the p - x plane. Shown are only the adiabats that pass through "1". The two adiabats are tangent and have the same second derivative at "1".

$$p_2 > p_1, \tag{2.15a}$$

$$x_2 < x_1, \tag{2.15b}$$

$$V_2 < V_1. \tag{2.15c}$$

Then, from the graph shown in Fig. 3 and the relation Eq. (2.12), one observes that the slope of the chord connecting "1" to "2" is just $-(j^2)$. Therefore, one can conclude [see Eq. (2.15)]:

$$u_2 < u_1, \tag{2.16a}$$

$$u_1 \geq u_{s1} (\propto \text{tangent at "1"}), \tag{2.16b}$$

$$u_2 \leq u_{s2} (\propto \text{tangent at "2"}). \tag{2.16c}$$

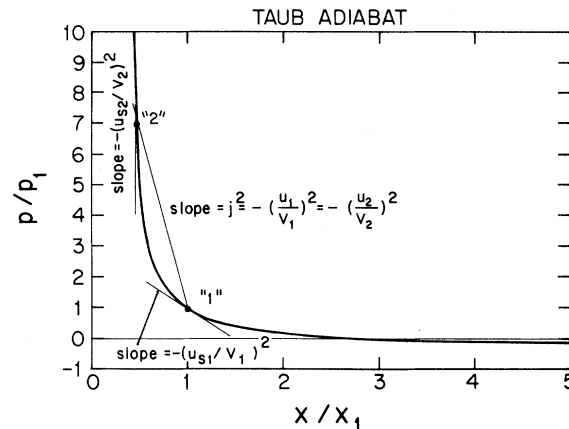


FIG. 3. Taub adiabat for a shock wave. The front side of the wave is in condition "1", the rear side in condition "2", and the slope of the chord between them is the negative of the square of the baryon flux. The slope at "1" and "2" can be used to determine the speed of sound in the respective fluids.

A weak shock corresponds to the situation where "2" lies only slightly above "1" on the adiabat. As the shock gets weaker, "2" approaches "1" and

$$u_1 \rightarrow u_{s1}, \quad u_2 \rightarrow u_{s2}, \quad (2.17)$$

i.e., the shock waves approach a sound wave as expected. As the shock becomes stronger, u_1 increases, but, surprisingly, u_2 decreases. From Landau and Lifshitz² one knows that

$$\beta_1 = \left(\frac{(p_2 - p_1)(e_2 + p_1)}{(e_2 - e_1)(e_1 + p_2)} \right)^{1/2}, \quad (2.18)$$

$$\beta_2 = \left(\frac{(p_2 - p_1)(e_1 + p_2)}{(e_2 - e_1)(e_2 + p_1)} \right)^{1/2},$$

so that for a highly relativistic fluid, $p = e/3$, and a very strong shock (e approaching infinity), the velocities become

$$\beta_1 \rightarrow 1, \quad \beta_2 \rightarrow \frac{1}{3} \quad (< v_s = 1/\sqrt{3}). \quad (2.19)$$

At first this result seems inconsistent with the analysis of the adiabat curve in Fig. 3 since both the slope of the chord, which gives β_2 , and the tangent at "2", which gives v_{s2} , approach infinity as the shock grows stronger ("2" moves further up the adiabat). However, in both cases the slopes go to infinity because the specific volume on the "2" side is going to zero; although both slopes approach infinity, their ratio is

$$\frac{\beta_2}{v_{s2}} \rightarrow \frac{1}{\sqrt{3}}. \quad (2.20)$$

Therefore the Taub-adiabat analysis is consistent.

The results can also be plotted using Eq. (2.14) (see Fig. 4). The plot yields β_1 in terms of β_2 and contains a larger range of solutions than is physically applicable. For example, for $\beta_2 < \frac{1}{3}$, β_1 is greater than one and this is not possible. The region in which $\beta_2 \geq 1/\sqrt{3}$ means that β_2 is greater than v_{s2} which is bounded in the highly relativistic limit by $c/\sqrt{3}$. By Eq. (2.16c) this cannot be satisfied by a shock wave. The physically interesting region is the intermediate one which begins at $\beta_2 = 1/\sqrt{3}$ for a weak shock and terminates at $\beta_2 = \frac{1}{3}$ for a strong shock. For a shock wave, the velocity of the fluid at the rear of the wave is always subsonic with respect to the wave front. These curves represent an alternative to the conventional Taub-adiabat analysis in which the continuity condition has not been utilized.

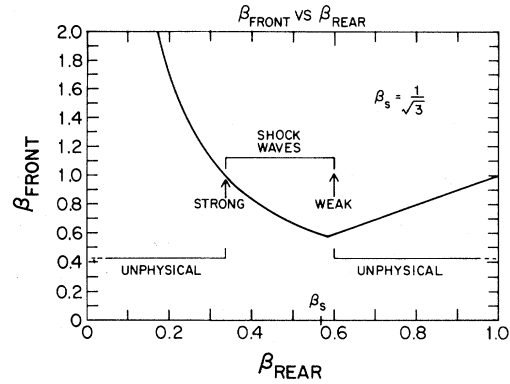


FIG. 4. A plot of β_1 vs β_2 for a shock. Only the middle section of the curve for $\frac{1}{3} < \beta_2 < 1/\sqrt{3}$ is physically relevant.

III. RELATIVISTIC DETONATION WAVES

The analysis of detonation waves proceeds in close analogy to the analysis of shock waves. The expressions governing a detonation-wave propagation can also be expressed in terms of e and p , permitting application of these results to fluids obeying a general equation of state. For purely pedagogical reasons, a specific form for the equation of state will be presumed. In particular, it will be assumed (1) that both the burnt and the unburnt fluid are in thermal equilibrium and (2) that the temperature is so high that the fluids are highly relativistic. Assumption (1) really has two parts: first it is assumed that the unburnt fluid is in thermal equilibrium, which is a matter of choice of initial conditions; second, it is assumed that the burnt fluid is also in thermal equilibrium which is an assumption about the dynamics of the fluid after combustion. Assumption (2) is (initially) an example that is as far removed from the zero-temperature case as possible. It is a trivial process to recover the expressions for general e and p from the relations that will be derived.

The assumptions can be condensed into the expression

$$p_{\text{thermal}} = \frac{1}{3} e_{\text{thermal}} = \frac{1}{3} a T^4. \quad (3.1)$$

As the temperatures T_i , $i = 1, 2$ on either side of the wave approach infinity, Eq. (3.1) becomes a valid approximation. To distinguish this case from a shock wave, there is an additional stored energy ϵ in fluid "1" which is released as the wave front passes. The energy density on either side is therefore

$$e_1 = aT_1^4 + \epsilon, \tag{3.2}$$

$$e_2 = aT_2^4. \tag{3.3}$$

Conservation of energy implies

$$\frac{d}{dt}(eV) = -p \frac{dV}{dt}, \tag{3.4}$$

where V is a volume of fluid element. The assumption that e and p depend on the temperature T and no other thermodynamic variables means

$$\mathcal{F}_1 = \text{diag}(\frac{1}{3}aT_1^4 - \epsilon, \frac{1}{3}aT_1^4 - \epsilon, \frac{1}{3}aT_1^4 - \epsilon, aT_1^4 + \epsilon), \tag{3.6a}$$

$$\mathcal{F}_2 = \text{diag}(\frac{1}{3}aT_2^4, \frac{1}{3}aT_2^4, \frac{1}{3}aT_2^4, aT_2^4). \tag{3.6b}$$

Transforming both expressions to the frame in which the shock front is stationary and equating them on both sides of the discontinuity results in the fundamental equations of equilibrium for the detonation wave:

$$\frac{4}{3}u_2\gamma_2aT_2^4 = \frac{4}{3}u_1\gamma_1aT_1^4, \tag{3.7a}$$

$$(\frac{4}{3}u_2^2 + \frac{1}{3})aT_2^4 = (\frac{4}{3}u_1^2 + \frac{1}{3})aT_1^4. \tag{3.7b}$$

The continuity equation (2.11) is unchanged for the detonation wave.

Because all the equations for the detonation wave have the same form as the case for the shock wave (the only difference is the addition of ϵ to the expression for the pressure and energy density on the "1" side), the adiabat equation (2.13) is still valid; the equation can be reexpressed as

$$(p_2 + \frac{1}{3}p_1)(x_2 - \frac{1}{3}x_1) = \frac{8}{9}x_1p_1 + \frac{4}{3}\epsilon x_1. \tag{3.8}$$

However, in plotting the one-parameter family corresponding to the possible states "2", the curve does not pass through the given initial point "1" as it did for the shock adiabat (see Fig. 5). The new curve is referred to as the detonation adiabat. The fact that the shock adiabat passes through the point "1" is due to the fact that e_1 and e_2 are the same functions of p_1 and p_2 , respectively, whereas this does not now hold on account of the chemical difference between the two fluids.

In Eq. (3.8), the shock adiabat, corresponding to $\epsilon=0$, passes through the point (p_1, x_1) and is a hyperbola with asymptotes along $p = -p_1/3$ and along $x = x_1/3$. The detonation adiabat has the same asymptotes but a greater major axis D between the center of the hyperbola $(-p_1/3, x_1/3)$ and the nearest point on the curve. In general the expression for D is

that adiabaticity can be assumed. For a small adiabatic increase in V , the temperature of particles behaves like $V^{-1/3}$. The stored energy, however, is independent of V . Therefore, the pressure in fluid "1" is

$$p_1 = \frac{1}{3}aT_1^4 - \epsilon \tag{3.5}$$

and the energy-momentum tensor in the rest frame of each fluid is

$$D = \frac{16}{9}x_1p_1 + \frac{8}{3}\epsilon x_1 \tag{3.9}$$

which increases monotonically with increasing ϵ . In Fig. 6, various adiabats as a function of ϵ are shown. The greater ϵ is, the greater the distance between the shock adiabat and the detonation adiabat.

The previous formula, Eq. (2.12), for the baryon flux density is still valid (independent of ϵ); its square is the negative of the slope of the chord connecting "1" (on the shock adiabat) to "2" (on the detonation adiabat). From Fig. 5 one observes that $-j^2$ cannot be less than the slope of the

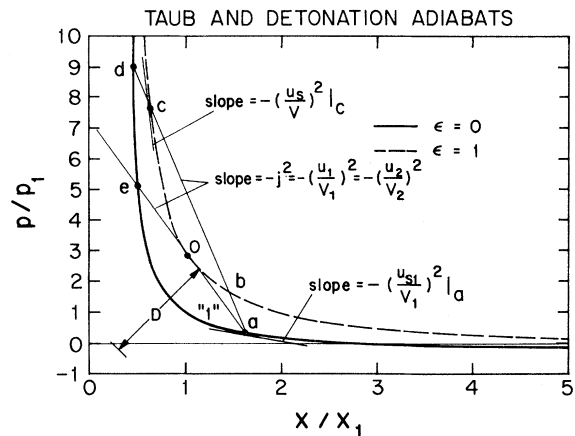


FIG. 5. Shock and detonation adiabats for the case where the unburnt fluid is "1" and the burnt fluid lies on the dashed curve about the point 0 (e.g., c). The line from "1" to 0 corresponds to the Jouget line. The line a-b-c-d represents a detonation with a larger jump in entropy than the Jouget line. D is the major axis of the hyperbola through "1" and the major axis of the hyperbola through 0.

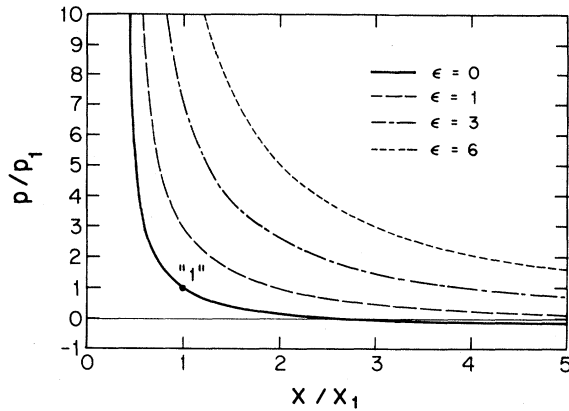


FIG. 6. Various detonation adiabats as a function of the vacuum energy ϵ . The curves have the same asymptotes but the major axis D increases with increasing ϵ .

tangent line between the point (p_1, x_1) and the point 0 on the detonation curve. The flux j is just the number of baryons which are ignited per unit time per unit area of the surface of the detonation wave. For a fixed (nonzero) ϵ one finds that this quantity must be above a certain limiting value.

The forward front of the detonation wave is a true shock wave in the unburnt fluid "1". The fluid is compressed and heated to a state represented by the point d (see Fig. 5) on the shock adiabat of fluid "1". The chemical reaction begins in the compressed gas and as the reaction proceeds, the state of the gas is represented by a point which moves down the chord da (the baryon flux is constant). Heat is evolved, the fluid expands, and its pressure decreases; this continues until the combustion is complete and the whole heat of the reaction has been evolved. The corresponding point on the adiabat is c , which represents the final state of the combustion products. (The lower point b at which the chord ad intersects the detonation adiabat cannot be reached if the reaction is exothermic.) Thus, the detonation is represented by the part of the detonation adiabat lying above the point 0.

Since the tangent to either curve at a point (p, x) is related to the speed of sound in the medium corresponding to that point, one observes from the above analysis and from Fig. 5 that ($\beta_{si} \equiv v_{si}$)

$$\beta_2 \leq \beta_{s2}, \quad (3.10)$$

i.e., a detonation wave moves relative to the fluid behind it with a velocity less than or equal to the speed of sound in that fluid; the equality holds for the point 0 which is referred to as the Jouget point. The velocity of the detonation wave with respect to fluid "1" is always supersonic (as can be seen from Fig. 5):

$$\beta_1 > \beta_{s1}. \quad (3.11)$$

The velocity with which the detonation wave moves with respect to the unburnt gas "1" (β_1) is referred to as the *velocity of propagation of the detonation wave*. The difference $\beta_1 - \beta_2$ is the velocity of the combustion products relative to the unburnt gas and is always positive.

From the analysis of the Poisson adiabats, the curves of constant entropy, one can also conclude that the entropy in fluid "2" is a minimum for the case of the chord which traverses point 0. The change in entropy from fluid "1" to fluid "2" is a maximum for the same chord. For these reasons, the Jouget point is a special point on the detonation adiabat.

If the shock wave from the detonation is due to the combustion process itself (and is not produced by some external source), it has been argued that the detonation must correspond to the Jouget point.² The velocity of the detonation wave relative to the combustion products just behind it (β_2) is exactly equal to the speed of sound while the velocity relative to the unburnt fluid has its least possible value. This hypothesis was first put forward by Chapman and Jouget (see Ref. 2) and is referred to as the *Chapman-Jouget condition*. One case in which the hypothesis can be proven is for a spherical detonation wave caused by the combustion process. The Chapman-Jouget condition will be presumed for the moment and justified at the end of this section.

An alternative way to represent the results is to plot the fluid velocities in the front and rear of the shock wave directly as a function of ϵ . If e is the thermal energy, the explicit expressions for β_1 and β_2 are (in the highly relativistic limit)

$$\beta_1 = \frac{1}{\sqrt{3}} \left[\frac{e_2 + \frac{1}{3}e_1 - \epsilon}{e_1 + \epsilon + p_2} \right]^{1/2}, \quad \beta_2 = \frac{1}{\sqrt{3}} \left[\frac{e_1 + \epsilon + \frac{1}{3}e_2}{e_2 + \frac{1}{3}e_1 - \epsilon} \right]^{1/2}. \quad (3.12)$$

One can also compute the equation for β_1 vs β_2 in the highly relativistic limit ($p = e/3$):

$$\beta_1 = \frac{(1/6\beta_2 + \frac{1}{2}\beta_2) + [(1/6\beta_2 + \frac{1}{2}\beta_2)^2 + \alpha^2 + \frac{2}{3}\alpha - \frac{1}{3}]^{1/2}}{1 + \alpha} \tag{3.13}$$

Using the Chapman-Jouget condition $\beta_2 = \beta_{s2} = 1/\sqrt{3}$, one finds

$$\beta_1 = \frac{1/\sqrt{3} + (\alpha^2 + \frac{2}{3}\alpha)^{1/2}}{1 + \alpha}, \tag{3.14}$$

where $\alpha = \epsilon/aT_1^4$ measures the ratio of the vacuum energy to the thermal energy for the unburnt fluid. Plots of β_1 vs β_2 for various values of α are shown in Fig. 7. In the limit that $\epsilon \rightarrow 0$, the curves approach the curve corresponding to a shock wave (Fig. 4), as one expects. The Chapman-Jouget condition fixes $\beta_2 = 1/\sqrt{3}$, which, in the limit of $\epsilon \rightarrow 0$, implies $\beta_1 = 1/\sqrt{3}$. This result shows that the limit of a weak detonation wave is the same as the limit of a weak shock wave, although from the adiabat curves it can be seen that the limits are from different directions. As ϵ increases, the detonation wave grows strong and, from the adiabat curves, one can see that the detonation wave acts less and less like a shock wave. From Fig. 7 one observes that, with the Chapman-Jouget condition imposed, β_1 increases as ϵ increases and the velocity of the detonation wave with respect to the unburnt fluid becomes supersonic. The dependence of β_1 —which is also the velocity of the detonation wave front—on α is shown in Fig. 8(a). For T_1 strictly zero (α approaches infinity), Eq. (3.7b) is impossible to satisfy because the left-hand side of the equation is negative. Therefore, no equilibrium front can even be established. The positive pressure on the rear side of the detonation wave and

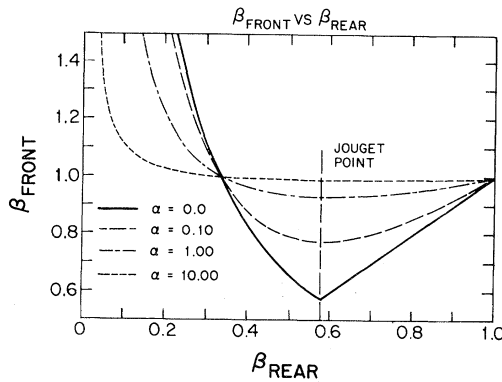


FIG. 7. β_1 vs β_2 for a detonation wave as a function of $\alpha = \epsilon/(e_1 \text{ internal})$, where, in the relativistic case, $(e_1 \text{ internal}) = aT_1^4$. The Jouget condition fixes $\beta_2 = 1/\sqrt{3}$. As α increases, β_1 approaches unity.

the negative pressure on the front side lead to a rapidly accelerating detonation wave whose velocity approaches the speed of light. If T_1 is nonzero the velocities of the fluids can always be adjusted to find an equilibrium solution. In Fig. 8(b) is shown T_2/T_1 , the ratio of the temperature of the burnt fluid to that of the unburnt fluid vs α , as derived from (3.7b). The ratio of temperatures is only weakly dependent on α in the relativistic limit.

A case of particular interest is the spherical detonation wave centered about the point where the fluid is first ignited. In this case one can analyze the fluid within the detonation wave (as well as along the detonation front). It will be assumed that the radius of the detonation wave is so large that equilibrium has been achieved and the wave front can be treated as (locally) planar. Since the fluid must be at rest in front of the detonation wave (by symmetry) the fluid velocity must de-

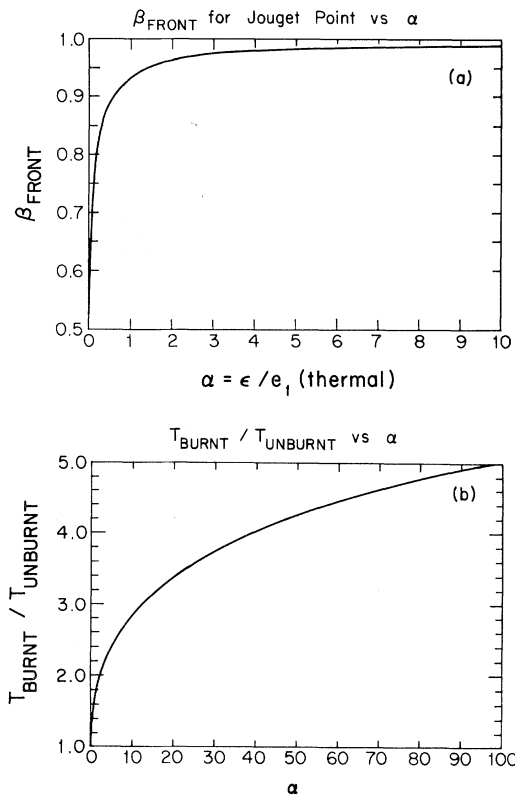


FIG. 8. (a) β_1 vs $\alpha = \epsilon/(e_1 \text{ internal})$, where in the highly relativistic case $(e_1 \text{ internal}) = aT_1^4$. (b) T_2/T_1 vs α in the highly relativistic limit.

crease from the detonation wave towards the center. Because there is no distance parameter, the flow must be able to be described in terms of the ratio between the distance from the center of the wave and the time t : $\xi = r/t$. The variable ξ has the units of velocity and represents the velocity of a given point in the detonation wave profile. The particles at the point described by ξ in the wave profile move with a (different) velocity v . Near the detonation front $\xi = \beta_1$ and at the center of the wave $\xi = 0$.

In order to describe the dynamics of the detonation wave, the equations of motion are required for the case of spherically symmetric flow. The relativistic version of the continuity condition is given by (in units where $c = 1$)

$$\frac{\partial(n\gamma)}{\partial t} + \frac{\partial(nv\gamma)}{\partial r} + \frac{2(nv\gamma)}{r} = 0. \quad (3.16)$$

The equation of conservation of entropy is

$$\frac{\partial\sigma}{\partial t} + v \frac{\partial\sigma}{\partial r} = 0, \quad (3.17)$$

where σ is the entropy per baryon. And Euler's equation is

$$\frac{\partial v}{\partial t} + v \frac{\partial v}{\partial r} = -\frac{1}{w\gamma^2} \left[\frac{\partial p}{\partial r} + v \frac{\partial p}{\partial t} \right]. \quad (3.18)$$

The equations may be rewritten in terms of the variable ξ :

$$\frac{n'}{n}(\xi - v) = v' + \frac{2v}{\xi} - \gamma^2 v v'(\xi - v), \quad (3.19a)$$

$$(\xi - v)\sigma' = 0, \quad (3.19b)$$

$$(\xi - v)v' = \frac{1}{w\gamma^2}(1 - v\xi)p', \quad (3.19c)$$

where primes indicate derivatives with respect to ξ . By the first relation, ξ cannot equal v without contradiction. Therefore, the entropy relation implies $\sigma' = 0$ —entropy is conserved. Therefore, $p' = (\partial p / \partial e)_s e' = v_s^2 e'$, where v_s is the speed of sound (which is also a function of ξ). Equation (3.19c) therefore implies

$$\left[\gamma^2 \frac{(\xi - v)}{1 - v\xi} \right] v' = v_s^2 \frac{e'}{w}. \quad (3.20)$$

By Eqs. (2.3) and (2.4), the right-hand side of Eq. (3.20) can be rewritten

$$\frac{e'}{w} = \frac{n'}{n}. \quad (3.21)$$

The right-hand side can then be reexpressed using

Eq. (3.19a):

$$\left[\gamma^2 \frac{(\xi - v)^2}{v_s^2(1 - v\xi)} - [1 - \gamma^2 v(\xi - v)] \right] v' = \frac{2v}{\xi} \quad (3.22)$$

which is the central equation describing the velocity profile within the detonation wave. Unfortunately, the equation is too difficult to integrate analytically, but its important properties can be discerned without much difficulty.

It is first useful to consider the conditions under which the fluid velocity v is zero. For $\xi \approx \beta_2$ corresponding to a point in the wave profile near the outer part of the wave, v is nonzero. As ξ decreases, v decreases to zero and $\ln v$ tends to $-\infty$. Therefore, $d(\ln v / d\xi)$ should be expected to go to $+\infty$. For small v , Eq. (3.22) implies

$$\frac{d \ln v}{d\xi} = \frac{2v_s^2}{\xi(\xi^2 - v_s^2)}, \quad (3.23)$$

the left-hand side of the equation approaches infinity for $\xi = 0$ or $\xi = v_s$. At the origin $\xi = 0$, the fluid is at rest by symmetry. There is a region between $\xi = 0$ and $\xi = v_s$ inside the detonation wave for which the fluid is at rest. [Equation (3.22) breaks down in this region.] The sphere $\xi = v_s$ in fact corresponds to a wave of profile velocity $\xi = v_s(0)$ where $v_s(0)$ is the velocity of sound for the fluid at rest near the center of the detonation wave (since, as noted before, v_s is generally a function of ξ).

Near the point $v = 0$ and $\xi = v_s(0)$, Eq. (3.24) can be linearized to yield the velocity profile $v(\xi)$:

$$v \frac{d\xi'}{dv} = \xi' - v [1 - v_s^2(0)] - [v_s - v_s(0)], \quad (3.24)$$

where $\xi' = \xi - v_s(0)$. The quantity $[v_s - v_s(0)]$ is a function of ξ , or, alternatively, for small v , a function of v . The simplest assumption is that, for small r , it is proportional to v . If it is a higher power of v it can be ignored in the computation. Equation (3.24) can be reexpressed in the form

$$v \frac{d\xi'}{dv} - \xi' = -\alpha_0 v \quad (\alpha_0 = \text{const}), \quad (3.25)$$

which has solutions [by substituting $\xi' = v f(v)$]

$$\xi' = \alpha_0 v \ln \left[\frac{v_0}{v} \right] \quad (v_0 = \text{const}). \quad (3.26)$$

The result shows that near the inner boundary point $v = 0$ (a) the curve $v(\xi)$ has a horizontal tangent, and (b) the first derivative of the profile is

continuous but all higher derivatives are infinite.

Note also that for small v , Eq. (3.26) implies

$$\xi - v - v_s = \xi' - v - [v_s - v_s(0)] \tag{3.27a}$$

$$= \alpha_0 v \left[\ln \left(\frac{v_0}{v} \right) - 1 \right] \tag{3.27b}$$

which is positive. It will be shown that $\xi - v - v_s$ cannot change sign anywhere in the region of flow considered. Consider a point (if there is one) where

$$\mu = \frac{\xi - v}{1 - v\xi} = v_s, \quad v \neq 0 \tag{3.28}$$

for this value, the coefficient of v' in Eq. (3.22) is zero and so v' must be infinite at such a point. Using the equations above, the second derivative can be shown to be finite at such a point:

$$v'' \propto -v/\xi. \tag{3.29}$$

This means that ξ as a function of v has a maximum at such a point. The function $v(\xi)$ only is physical for ξ less than the value corresponding to condition (3.28) and this, it will be shown, corresponds to the outer boundary of the solution. If $\mu = v_s$ only at the outer boundary and $\mu > v_s$ for small v [see Eq. (3.27b) near the inner boundary], Eq. (3.29) implies that

$$\mu = \frac{\xi - v}{1 - v\xi} > v_s \tag{3.30}$$

everywhere between the two boundaries. Evaluated at the detonation wave front, the velocity μ is just the velocity of the fluid behind the front relative to ξ , the profile velocity of the front itself. A surface on which $\mu > v_s$ cannot be the front of a detonation wave, by Eq. (3.10), however, so the outer boundary of the region must correspond to the detonation front. On this boundary, v falls from its maximum value discontinuously to zero and the velocity of the boundary relative to the gas is just equal to the velocity of the front of the detonation-wave profile—the local velocity of sound (see Fig. 9). The detonation wave therefore must correspond to the Jouget point.

The detonation wave has behind it, therefore, a spherical similarity rarefaction wave in which the velocity decreases monotonically at the inner discontinuity to zero. The density and pressure can be shown to decrease monotonically also (although they do not decrease to zero) at the inner boundary and then are constant within that radius. The fluid within the inner boundary is therefore at

rest with respect to the unburnt fluid and at finite temperature, pressure, and density. The width of the “slim” layer between the inner and outer boundaries generally grows as a fraction of time since the velocity of sound in the inner fluid (= speed of inner boundary) is less than the velocity of sound near the fluid front (= velocity of the detonation wave front). (In the extreme relativistic limit the slim thickness remains roughly constant.) The volume of inner fluid grows like $[v_s(0)t]^3$.

IV. BUBBLES GROWTH IN FALSE VACUUM DECAY

False vacuum decay refers to a phenomenon in field theory in which a system is trapped in a metastable phase and must decay through barrier penetration into the stable phase. As stated in the Introduction, Coleman has analyzed the decay process for a system that is truly a vacuum and at zero temperature using the semiclassical approximation. He derived a picture of the decay process that is like the classical description of a first-order phase transition of which the process he studied is the quantum analog.

According to Coleman’s results, the decay occurs through the nucleation of numerous bubbles in the metastable system inside of which is the stable phase. If the bubbles that are nucleated are above a certain critical size, they begin to grow, accelerating very rapidly. For his solution in a vacuum at zero temperature, Coleman was able to explicitly show that the space-time path of a point on the bubble wall follows a hyperbolic world line in which it continually accelerates, rapidly approaching the light cone. The force for accelerating the wall comes directly from the process of converting

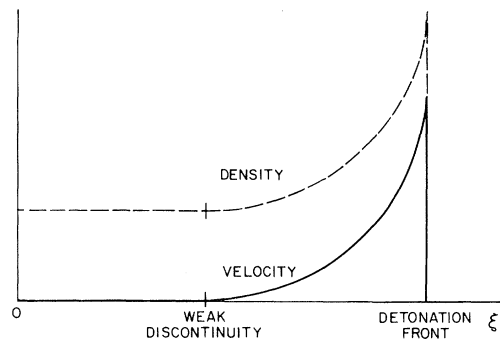


FIG. 9. Velocity profile as a function of $\xi = r/t$ for a detonation wave.

the metastable phase to the stable one.

From the discussion of a detonation wave in Sec. III it is strongly suggested that the growth of a bubble at *fixed* temperature should be very similar to the growth of a spherical detonation wave. Both the spherical detonation wave and the bubble begin at rest and begin to accelerate due to greater pressure inside than outside. In both cases, the acceleration of the front is due to the energy derived from converting outside "fluid" into inside "fluid." In the case of the bubble the physics inside the bubble may be different from the physics outside (symmetries may be broken for example), just as in the case of the detonation wave the chemistry of the unburnt fluid is different from the chemistry of the burnt fluid. The acceleration of the fronts continues until the pressure on the outside of the fronts becomes great enough to just counterbalance the pressure on the inside. If the fronts move any faster, they are slowed by the pressure on the outside; if they move any slower, they are speeded up by the pressure on the inside. The equilibrium front is therefore established.

For a finite-temperature effective potential $V(\phi)$ that has a local (false) minimum at ϕ_0 and a global (true) minimum at ϕ_1 , ϵ is given (approximately) by $V(\phi_0) - V(\phi_1)$. When the bubble is first produced, the value of the field far from the center of the bubble is near ϕ_0 ; in the center of the bubble the value of the field is ϕ'_0 , where $\phi_0 < \phi'_0 < \phi_1$ (where we choose ϕ_1 to be greater than ϕ_0). As the bubble grows, the value of the field inside the bubble approaches ϕ_1 and remains near that value. The analogy of the bubble to the spherical detonation wave should be appropriate when this approximate "equilibrium" condition is reached.

The analogy should be valid provided that particles outside the bubble wall interact strongly with the bubble wall. For a bubble in a scalar field theory, the bubble wall consists of a coherent superposition of scalar particles. Scalar excitations of the false phase must interact with the walls to produce excitations of the true phase. Fields that couple strongly to scalar particles (such as gauge mesons) should also interact strongly with the scalar particles in the bubble wall. In such cases, the detonation-wave analysis should be useful.

There is generally no conservation law or continuity condition since scalar excitations are generally produced as the wall passes. Nevertheless, the energy and momentum conservation laws [Eqs. (3.7a) and (3.7b)] are still valid. Therefore Eqs. (3.13) and (3.14) are still applicable, and Figs. 7

and 8 can still be utilized. For decay in the presence of conserved charges, the adiabat condition Eq. (3.8) should be applied in addition.

It is pleasing to note that, in the limit of zero temperature [see Eq. (3.14) for $\alpha \rightarrow \infty$] the results for the detonation wave match up nicely with the results that Coleman found. As discussed in Sec. III, in the limit $T_1 \rightarrow 0$ the pressure on the outside of the front is negative definite and an equilibrium front can never be achieved; the wave front accelerates rapidly forever, approaching the speed of light. For any finite temperature, however, the fluid velocities can be adjusted so that there exists an equilibrium front.

Assuming the analogy between the bubble and the detonation wave is correct, the results of Sec. III for β_1 vs β_2 can be used to give the bubble-wall velocity as a function of the temperature [using Eq. (3.14)] when the temperature inside and outside the bubble is much greater than the scale of masses. Depending on the temperature, the velocity of the bubble wall can vary between $c/\sqrt{3}$ in the limit of high temperatures and c as the temperature approaches zero. Also, unlike the case at zero temperature, bubbles at finite temperature would be expected to leave behind the bubble wall some small fraction of the bubble energy which is at rest with respect to the bubble wall at some fixed temperature.

If the transition is from a metastable symmetric phase to a stable symmetry-breaking phase, then some gauge mesons can gain a large mass in traveling from the outside to the inside of the bubble. It is interesting to consider what happens if such mesons dominate the energy density of the bubble interior so that the interior fluid must be treated as a nonrelativistic fluid. In this case, all equations of the previous section hold except

$$e_2 = \bar{a}T_2^3, \quad p_2 = 0. \quad (4.1)$$

In this case, solving the same equations one finds

$$\beta_1 = \frac{\beta_2 + [\beta_2^2 + 3(1+\alpha)(\frac{3}{4}\alpha - \frac{1}{4})]^{1/2}}{\frac{3}{2}(1+\alpha)}. \quad (4.2)$$

The velocity β_2 must equal the speed of sound in the (nonrelativistic) fluid "2", β_{s2} . The solution for velocity β_1 is only valid, though, for $\beta_1 > \beta_{s1}$, where β_{s1} is the velocity of sound in the outside relativistic fluid. In general, $\beta_{s1} > \beta_{s2}$, so Eq. (4.2) is only valid for $\alpha > \frac{1}{3}$. For $\alpha < \frac{1}{3}$, the pressure of the unburnt fluid is greater than the pressure of the burnt fluid and the bubble collapses. (The

pressure inside the bubble is reduced because most of the energy of the transition is stored in the mass of the gauge mesons.) As $\alpha \rightarrow \infty$, β_1 approaches unity, as before. The result is surprising because, for $\alpha < \frac{1}{3}$ at fixed T , such a system can produce no growing bubble even though $\epsilon > 0$. (As the system supercools, bubbles only appear after $\alpha > \frac{1}{3}$.)

The opposite case, where the metastable phase is symmetry breaking and the stable phase is symmetry preserving, is also interesting. In this case, the results of Sec. III are correct except that

$$e_1 = \tilde{\alpha} T_1^3, \quad p_1 = 0, \quad (4.3)$$

where the unburnt fluid outside the bubble is treated as nonrelativistic. In this case, β_1 can be shown to be

$$\beta_1 = \frac{\sqrt{3}/2 + (\frac{3}{4} + 4\tilde{\alpha} + 4\tilde{\alpha}^2)^{1/2}}{2(1 + \tilde{\alpha})}, \quad (4.4)$$

where $\tilde{\alpha} = \epsilon/\tilde{\alpha} T_1^3$ (a different form but with the same interpretation as before) and β_2 for the relativistic interior fluid has been assumed to be $1/\sqrt{3}$. In this case there is a valid equilibrium for all $\tilde{\alpha}$:

$$\frac{\sqrt{3}}{2} < \beta_1 < 1 \quad \text{for } 0 < \tilde{\alpha} < \infty. \quad (4.5)$$

The pressure exterior to the bubble is reduced due to the mass of the gauge mesons so that the equilibrium velocity of the bubble is greater than if the outside fluid were relativistic.

Of course, the energy density and pressure have contributions from both the massless and massive excitations. These results in extreme limits only serve to show the range of possible behaviors for the bubble.

The results stated in the last paragraphs are in opposition to the conventional assumptions that have been used in analyzing first-order phase transitions in the early Universe. First, it is assumed that once the bubbles are produced, they grow at the speed of light. Since the region outside the bubbles is expanding due to effects of general relativity, it is important to know the speed of growth of the bubbles to know if they can grow large enough for them to coalesce before the regions outside them grow too large. Under the cosmological conditions, as the outside regions expand, their temperature also *decreases*; the environment is therefore more complicated than was assumed in Sec. III. As the temperature on the outside drops, the bubble-detonation velocity increases until T_1 becomes negligible and the bubble velocity ap-

proaches the speed of light. Depending on the details of a field-theoretic model, however, the temperature may have to drop many orders of magnitude before the effects of finite temperature become negligible. Therefore, modifications in the rate of completion of first-order transitions should be considered.

In cases where the transition is completed, the bubbles grow more slowly than the speed of light before they coalesce. Unlike the conventional assumptions, the bubbles are not spacelike separated before the walls meet. In particular, massless gauge mesons can be transmitted from one bubble to another, possibly conveying information as to the orientation of the Higgs fields in isospin space. Such "communication" could lead to increased correlations in phase transitions to states of broken symmetry. Such a process could reduce, for example, the number of monopoles produced in cosmological first-order phase transitions.

Perhaps more importantly, one must reconsider cases in which the transition is never completed because the rate of growth of the outside regions is more rapid than the bubble nucleation rate and bubble growth rate combined. Such "inflationary" scenarios have been typically depicted^{9,10} as being unphysical because the bubbles never coalesce; as they grow, it is conventionally assumed that *all* the energy from the conversion along the bubble front is stored in the wall. The Universe cannot exist on the inside of a bubble because the inside is cold and empty, it is said.¹¹ However, until the temperature on the outside grows to be very small, the bubbles grow as stable detonation waves which, as discussed at the end of Sec. III, do leave behind a small fraction of the energy density inside the bubble. For a bubble of the size of our present Universe and for conversion energies typical of current grand unified models, the total energy from conversion is a fantastic sum—many, many orders of magnitude greater than that found in our observable Universe. If a small fraction of that energy is left behind at rest with respect to the bubble wall and in thermal equilibrium, it may be enough to account for the entropy found in the observable Universe.

V. CONCLUSIONS

The main purpose of this paper was to extend previously known results on relativistic shock waves to the case of relativistic detonation waves.

Perhaps some direct application of these ideas to combustion processes in cosmology will be possible.

The main motivation for the paper was to gain an understanding as to how bubbles nucleated in first-order phase transitions at high temperatures may grow. The application to cosmological scenarios has been only briefly discussed and has been intentionally indefinite because the results are highly model dependent. A more complete treatment of the cosmological application is being presently studied. The basic message, however, is that conventional assumptions about bubble growth at zero temperature should be modified in accordance with the analysis of Sec. III. The results

may be important in cosmological scenarios in which there are an insufficient number of bubbles to percolate the Universe. The results should also be equally applicable to the case where monopoles, rather than bubbles, serve as the nucleation sites for mediating the first-order phase transition.¹²

ACKNOWLEDGMENTS

The author would like to thank B. Halperin and G. Lasher for many useful discussions and suggestions in the course of this project. This work was supported by the U. S. Department of Energy under Contract No. EY-76-C-02-3071.

¹A. Taub, *Phys. Rev.* **74**, 328 (1948).

²L. D. Landau and E. M. Lifshitz, *Fluid Mechanics* (Pergamon, London, 1959). For a related discussion of relativistic detonation waves in magnetohydrodynamics, see M. Cissoko, *Ann. Inst. Henri Poincaré* **17**, 43 (1972). See also G. Lasher, *Phys. Rev. Lett.* **42**, 1646 (1979).

³M. H. Johnson and C. F. McKee, *Phys. Rev. D* **3**, 858 (1971).

⁴K. S. Thorne, *Astrophys. J.* **179**, 897 (1973).

⁵S. Coleman, *Phys. Rev. D* **15**, 2929 (1977).

⁶A. D. Linde, *Phys. Lett.* **70B**, 306 (1977).

⁷P. Steinhardt, *Nucl. Phys.* **B179**, 492 (1981).

⁸M. A. Sher, *Phys. Rev. D* **22**, 2989 (1980).

⁹A. Guth and E. Weinberg, *Phys. Rev. D* **23**, 876 (1981).

¹⁰G. Cook and R. T. Mahanthappa, *Phys. Rev. D* **23**, 1321 (1981).

¹¹E. Weinberg, in proceedings of the Johns Hopkins Particle Physics Conference, 1981 (unpublished).

¹²P. Steinhardt, *Nucl. Phys.* **B190**, 583 (1981); *Phys. Rev. D* **24**, 842 (1981).